

Impact Experiments of Gypsum-Glass Beads Mixtures Simulating Parent Bodies of Ordinary Chondrites Minami Yasui¹ and Masahiko Arakawa², ¹Organization of Advanced Science and Technology, Kobe University, e-mail: yasui@eps.nagoya-u.ac.jp. ²Graduate School of Science, Kobe University, e-mail: masahiko.arakawa@penguin.kobe-u.ac.jp.

Introduction: It is proposed that most of small asteroids are impact fragments produced by high speed impact among parent bodies. Many small asteroids observed currently are correlated with the meteorites of ordinary chondrites recovered on the earth, and it is natural that the meteorites are also the fragments of these small asteroids. Thus, the impact disruption plays a very important role in the origin of small asteroids followed by the formation of ordinary chondrite. The ordinary chondrites have the components of millimeter-sized round grains, so called chondrules, and submicron-sized dusts, so called matrix. It is supposed that the planetesimals forming the parent bodies of ordinary chondrites could be mainly composed of chondrules and submicron-sized dusts. So, it is interesting to examine the collisional disruption and re-accumulation process for the planetesimals forming the parent bodies of ordinary chondrites.

Therefore, we conducted impact experiments with porous gypsum-glass beads mixtures having the spherical shape with various diameters simulating chondrules, and examined the effect of chondrules on the ejecta velocity and the impact strength.

Experimental methods: Impact experiments were conducted by using one- and two-stage light gas gun set in Nagoya University. We prepared the target samples of porous gypsum mixed with glass beads having the diameter of 100 μm , 1 mm, and 3 mm. The volume fraction of glass beads was about 0.6 because that of chondrules in the ordinary chondrites is estimated to be about 0.65-0.75 [1]. We made the targets having a cylinder shape with a diameter of 30 mm and a height from 20 to 40 mm, and a cubic shape with a side length from 10 to 30 mm. The experimental condition is described as follows. In the case of single-stage gas gun, we used the nylon projectile having a spherical shape with a diameter of 10 mm and a mass of 0.5 g. The impact velocity ranged from 80 to 180 m/s. In the case of two-stage gas gun, we used the nylon projectile having a cylindrical shape with a diameter of 1.6 mm, a height of 2.5 mm and a mass of 7 mg. The impact velocity was about 4 km/s.

The collisional disruption was observed by using a high-speed digital video camera to measure the ejecta velocity. The frame rate was set to be from 3×10^3 to 1×10^4 frames/sec, and the shutter speed was set to 1 μs . The fragment velocities were analyzed using the snapshots taken by the camera. We especially obtained the antipodal velocity for the representative of fragment veloci-

ties in each shot. Each recovered fragment was weighted to construct the cumulative mass distribution and we studied the effect of glass beads on the impact strength.

Results: Ejecta velocity. In this study, we used a velocity of fragment ejected from an antipodal point as a representative of fragment velocities. Fig. 1 shows the relationship between the antipodal velocity, V_a , and the energy density, Q . The energy density Q is defined by a kinetic energy of projectile divided by a total mass of projectile and target. As a result, the V_a did not change with the target shape and the glass bead size. However, the V_a obtained for low-velocity collision was about 10 times larger than that obtained for high-velocity collision at the same energy density in the case of 100 μm beads target. From this graph, we can derive the empirical equations as follows,

$$V_{al} = 10^{-1.3} \cdot Q^{0.8}, \quad (1)$$

$$V_{ah} = 10^{-3.6} \cdot Q^{1.2}, \quad (2)$$

where the subscripts, l and h, mean low- and high-velocity collisions, respectively.

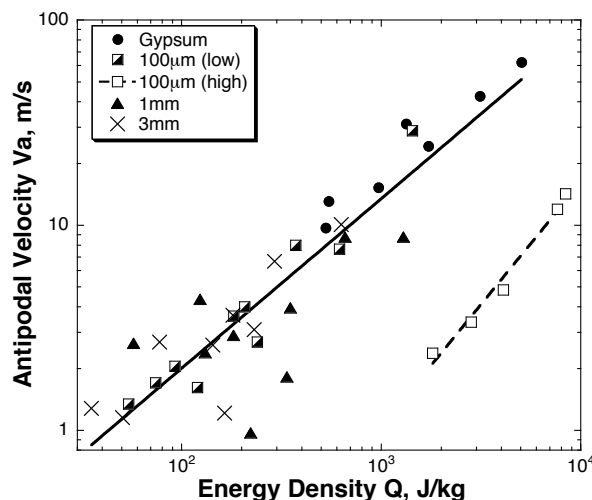


Figure 1: Antipodal velocity V_a vs. energy density Q . The solid line represents the fitting line for low-velocity collision using the Eq. 1, and the dashed line does that for high-velocity collision using the Eq. 2. The “low” and the “high” in the parentheses mean low- and high-velocity collisions, respectively.

Impact strength. Fig. 2 shows the relationship between the largest fragment mass normalized by the target mass, m_l/M_t , and the Q . The m_l/M_t did not change with the

target shape, however, it depends on the glass bead size and the impact velocity. This relationship can be fitted by the following power law relation,

$$m_1/M_t = 10^{q_0} \cdot Q^p, \quad (3)$$

where the parameters, q_0 and p , are summarized in Table 1 for all targets. The impact strength, Q^* , is defined as an energy density when the m_1/M_t equals to be 0.5 [2]. We calculated the Q^* using the Eq. 3, and the result for each target was listed on Table 1. In the case of low-velocity collision, the Q^* was smaller as the glass bead size was smaller. Furthermore, the Q^* for high-velocity collision was about five times larger than that for low-velocity collision in the case of 100 μm beads targets.

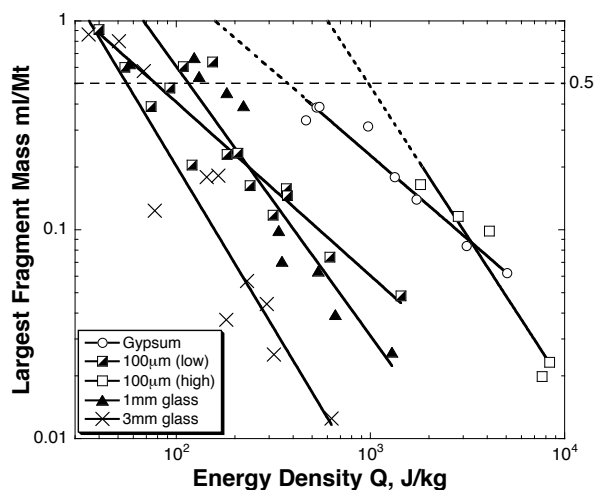


Figure 2: Largest fragment mass normalized by target mass m_1/M_t vs. energy density Q . The horizontal dotted line represents that the m_1/M_t is equal to be 0.5.

Discussion: As shown in the “Results” section, we found that the relationship between the V_a and the Q , and the Q^* were different between low- and high-velocity collisions, and furthermore, the Q^* depended on the glass bead size. In this section, we reanalyzed these results by using a non-dimensional impact stress, P_1 , and discussed the physical mechanism causing this difference and these dependences. The P_1 is defined as follows,

$$P_1 = \frac{\rho_t C_t V_a}{2Y_t}, \quad (4)$$

where ρ_t is the bulk density of target, C_t is the bulk sound velocity of target, and Y_t is the tensile strength of target [3]. We measured the bulk sound velocity using a pulse transmission method with ultrasonic acoustic wave and the tensile strength of targets by the Brazilian test [4]. Fig. 3 shows the relationship between the m_1/M_t and the P_1 . It is noticed that the only one relationship was appeared on the figure, irrespective of the glass bead size and the impact velocity, although in Fig. 2 there were five different

ones. Furthermore, our result was well consistent with that of porous gypsum obtained by Okamoto and Arakawa [5]. The empirical equation for our results and those by Okamoto and Arakawa could be obtained as the following equation,

$$\frac{m_1}{M_t} = 10^{-0.04 \cdot P_1 - 0.85}. \quad (5)$$

This result suggests that P_1 is a quite useful parameter to describe the degree of disruption for the target with different components and impacted at different velocities.

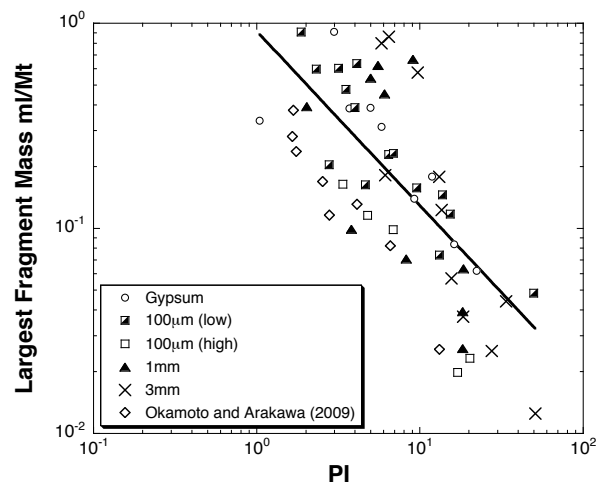


Figure 3: Largest fragment mass normalized by the target mass m_1/M_t vs. non-dimensional impact stress P_1 . The solid line represents the fitting line for gypsum and gypsum-glass beads mixture targets by using the Eq. 5.

Table 1: Parameters q_0 and p of Eq. 3, and impact strength Q^*

Target sample	q_0	p	Q^* [J/kg]
Gypsum	2.1	-0.9	446.1
100 μm (low- V)	1.3	-0.8	78.2
100 μm (high- V)	4.0	-1.4	978.3
1 mm	2.4	-1.3	115.8
3 mm	2.4	-1.6	55.7

References: [1] Grossman, J. N. et al. (1988) in *Meteorites and the Early Solar System*, Univ. of Ariz. Press, pp. 619-659. [2] Davis, D. R. and Ryan, E. V. (1990) *Icarus*, 83, 156-182. [3] Mizutani, H. et al. (1990) *Icarus*, 87, 307-326. [4] Mellor, M. and Hawks, I. (1971) *Emg. Geol.*, 5, 173-225. [5] Okamoto, C. and Arakawa, M. (2009) *Meteorit. Planet. Sci.*, 44, 1,947-1,954. [6] Arakawa, M. et al. (1995) *Icarus*, 118, 341-354. [7] Arakawa, M. (1999) *Icarus*, 142, 34-45.